CHEMISTRY
A European Journal

A Journal of
ChemPubSoc Europe

Accepted Article

Title: A New Drug Delivery System based on Tauroursodeoxycholic Acid and PEDOT

Authors: Stefano Carli, Giulia Fioravanti, Andrea Armirotti, Francesca Ciarpella, Mirko Prato, Giuliana Ottonello, Marco Salerno, Alice Scarpellini, Daniela Perrone, Elena Marchesi, Davide Ricci, and Luciano Fadiga

To be cited as: *Chem. Eur. J.* 10.1002/chem.201805285

Link to VoR: http://dx.doi.org/10.1002/chem.201805285

Supported by
ACES

WILEY-VCH

10.1002/chem.201805285

WILEY-VCH

A New Drug Delivery System based on Tauroursodeoxycholic Acid and PEDOT

Stefano Carli,* [a] Giulia Fioravanti,[a] Andrea Armirotti, [b] Francesca Ciarpella,[a],[c] Mirko Prato,[d] Giuliana Ottonello,[b] Marco Salerno,[d] Alice Scarpellini,[e] Daniela Perrone,[f] Elena Marchesi,[f] Davide Ricci,[a], [g] Luciano Fadiga[a],[c]

Abstract: Localized drug delivery represents one of the most challenging uses of systems based on conductive polymer films. Typically, anionic drugs are incorporated within conductive polymers through the electrostatic interaction with the positively charged polymer. Following this approach, the synthetic glucocorticoid Dexamethasone-phosphate is often delivered from neural probes to reduce the inflammation of the surrounding tissue. Encouraged by recent literature on the neuroprotective and anti-inflammatory properties of Tauroursodeoxycholic acid (TUDCA), we incorporated for the first time this natural bile acid within Poly(3,4-ethylenedioxythiophene) (PEDOT). We demonstrated that the new material PEDOT-TUDCA can efficiently promote an electrochemically controlled delivering of the drug, while preserving optimal electrochemical properties. Moreover, the low cytotoxicity observed with viability assays, makes PEDOT-TUDCA a good candidate for prolonging the time span of chronic neural recording brain implants.

[a] Dr. S. Carli, Dr. G. Fioravanti, Dr. F. Ciarpella, Dr. D. Ricci, Prof. L. Fadiga
Center for Translational Neurophysiology of Speech and Communication, *Istituto Italiano di Tecnologia*
44121 Ferrara (Italy)
E-mail: Stefano.carli@iit.it
[b] Dr. A. Armirotti and Dr. G. Ottonello
Analytical Chemistry Facility
Istituto Italiano di Tecnologia
16163 Genova (Italy)
[c] Dr. F. Ciarpella, Prof. L. Fadiga
Section of Human Physiology
University of Ferrara
44121 Ferrara (Italy)
[d] Dr. M. Prato and Dr. M. Salerno
Materials Characterization Facility
Istituto Italiano di Tecnologia
16163 Genova (Italy)
[e] Dr. A. Scarpellini
Electron Microscopy Facility
Istituto Italiano di Tecnologia
16163 Genova (Italy)
[f] Dr. D. Perrone and Dr. E. Marchesi
Department of Chemical and Pharmaceutical Sciences
University of Ferrara
44121 Ferrara (Italy)
[g] Dr. D. Ricci
DITEN
University of Genoa
16145 Genova (Italy)

Supporting information for this article is given via a link at the end of the document.

Introduction

The development of implantable microelectrodes, capable of recording and/or stimulating the neural activity, has revolutionized the field of neuroscience by enabling bidirectional communication with neural tissue at high spatial and temporal resolution.[1] Unfortunately, one of the main concerns related to chronically implanted microelectrodes is the adverse reaction of the surrounding tissue, which is known to progressively lead to the loss of neural recording/stimulating ability after few weeks post-implantation.[2] Thus, the modulation of the reactive tissue response represents one of the main goals to be reached in order to account for long-term use of neural implants. In this context, localized drug delivery from biocompatible poly(3,4-ethylenedioxythiophene) (PEDOT) based coatings on neural probes is one of the most powerful tool to reduce the foreign body response as well as to overcome the well-known issues related to the systemic administration of high dosage of anti-inflammatory drugs.[3] For this purpose, the use of potent synthetic anti-inflammatory Dexamethasone phosphate (DEX) is widely reported.[4] Typically, DEX is incorporated within conductive polymer films through electrostatic interactions, thereby leading to an electrochemically controlled drug-release system.[5] Very recently, we reported a new promising approach which is based on the chemical functionalization of PEDOT with Dexamethasone to provide a biochemically hydrolysable drug release system.[6]

Recent studies suggest that Tauroursodeoxycholic acid (TUDCA) may have cytoprotective and anti-apoptotic actions, with potential neuroprotective activity: TUDCA acts as a mitochondrial stabilizer and anti-apoptotic agent in several models of neurodegenerative diseases, including Alzheimer's, Parkinson's, and Huntington's diseases.[7] Moreover, anti-inflammatory properties of TUDCA toward acute neuroinflammation on an animal model have been reported: in particular, TUDCA exerts its anti-inflammatory activity by reducing microglial and astrocyte cells activation normally induced by neural devices implantation.[8] TUDCA is a hydrophilic bile acid that is produced by the liver and is widely used for treatment of acute and chronic liver diseases in humans.[9] Its structure is composed by ursodeoxycholic acid (UDCA) conjugated with taurine, through an amide bond, as depicted in Figure 1.

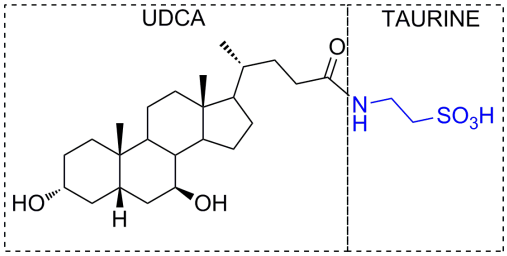

Figure 1. Chemical structure of TUDCA.

Surprisingly, to the best of our knowledge, drug delivery systems based on the incorporation of TUDCA within conductive polymers have not been reported hitherto, nor is its application as a potential anti-inflammatory agent for in vivo neural recording studies. Here, we incorporated for the first time TUDCA within a PEDOT backbone through the *ionic-approach*, which is expected to promote an electrochemically controlled delivery of the drug. Furthermore, we compared the new PEDOT-TUDCA composite with the *well-known* DEX-P conjugate (PEDOT-DEX) as far as both electrochemical and morphological properties are concerned. [4]

Results and Discussion

Electrodeposition and Electrochemical Characterization

According to the chemical structure of TUDCA (Figure 1), the SO_3^- group of the taurine unit can act as the dopant to counterbalance the positive charges of PEDOT during the anodic electrodeposition. It is worth noting that sulfonate based dopants, like paratoluene sulfonate (PTS) or polystyrenesulfonate (PSS), are among the most typically used counter ions to prepare stable and highly biocompatible PEDOT coatings.[10] The electrodeposition method adopted in this study was the cyclic voltammetry (CV), which was reported to provide improved film morphologies, with respect to galvanostatic and potentiostatic methods.[11] Figures 2a and 2b report the electrodeposition plots (first and last scan, respectively) of PEDOT-TUDCA. The onset of EDOT oxidation is cathodically shifted of 200 mV in presence of the sodium salt of TUDCA (TUDCA-SO_3Na, water solution), with respect to the less hydrophilic acidic form (TUDCA-SO_3H soluble in a 1:1 mixture of acetonitrile and water). This suggests that the film formation is strongly influenced by the operating conditions. In fact, it is known that the pKa values are solvent-dependent and, therefore, the ability of TUDCA to act as a dopant for PEDOT strongly depends on the extent of the dissociation of the sulfonate groups.[12] Moreover, a reduction of the oxidation potential of EDOT was observed in water, rather than organic solvents, due to a higher stabilization of the cationic oxidized monomer EDOT by the solvent.[13] The higher availability of free SO_3^- groups in water solution for TUDCA-SO_3Na reflects in a more effective doping during the electrodeposition that finally leads to lower impedance values (Figure S1) with respect to films obtained from TUDCA-SO_3H in ACN/water.

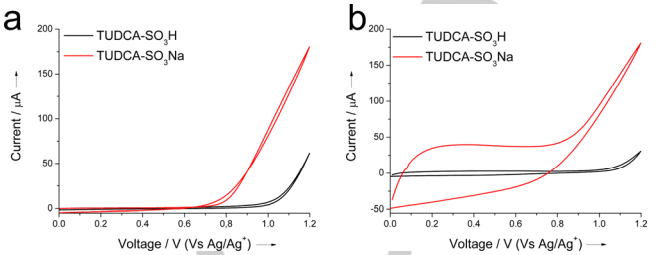

Figure 2. Typical a) first and b) last deposition plot, obtained with the acidic form of the bile acid (TUDCA-SO_3H) in 1:1 ACN/H_2O or with its sodium salt (TUDCA-SO_3Na) in H_2O, respectively. (0.01N EDOT and 0.02 N of TUDCA-SO_3H or TUDCA-SO_3Na).

CV analysis confirmed that TUDCA does not undergo any faradaic reaction and/or degradation that might compete or interfere with the oxidation of EDOT during the electrodeposition process (see Figure S2). For the sake of clarity, we will use hereafter the acronym PEDOT-TUDCA to refer to the composite electrodeposited from a deposition mixture containing the sodium salt of TUDCA (see experimental section for details). We compared the electrochemical properties of PEDOT-TUDCA films to those of PEDOT-DEX films prepared in the same conditions. The oxidation of EDOT is shifted by ~ 50 mV at lower overpotentials in the presence of TUDCA, with respect to DEX-P (as observed by the onset of the curve in Figure 3a).

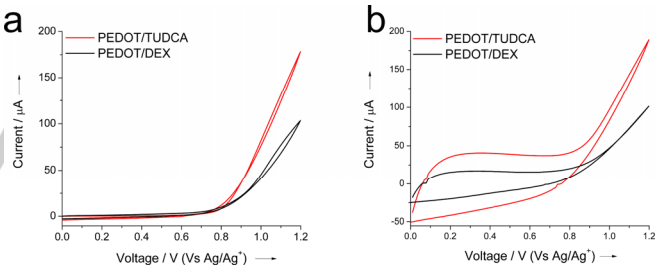

Figure 3. Typical a) first and b) last deposition plot for PEDOT-TUDCA and PEDOT-DEX, respectively.

An extra-stabilization of the oxidized EDOT, leading to a reduction of its oxidation potential, has been reported for electrodeposition in presence of surfactants.[13] It is also known that natural bile acids, including TUDCA, are biological surfactants involved in the solubilisation and absorption of dietary fat and lipid soluble endogenous molecules as well as hydrophobic drugs.[9,14] Moreover, the steeper oxidation curve (Figure 3a,b) as well as the more pronounced nucleation loop (see the typical trace crossing point during the reverse sweep reported in the first cycle deposition of Figure S3), are consistent with a kinetically favored electrodeposition of EDOT in presence of TUDCA, with respect to PEDOT-DEX film formation.[15] In fact, it is widely accepted that the mechanism of electropolymerization of five-membered heterocycles, including PEDOT, involves the coupling of two radicals to produce a dihydro oligomer di-cation which leads to an oligomer after loss

of two protons and re-aromatization.[16] Thus, the polymer growth at the electrode interface is dominated by the precipitation of oligomers that become insoluble in the electrolyte. The higher faradaic current exchanged during the deposition of PEDOT-TUDCA is in accordance with an improved film formation, in terms of higher thickness, higher charge storage capacity (CSC, Figure S4) and lower |Z| impedance (Figure S5). It is important to note that, for the sake of neural sensing, lower impedance represents the most desirable property in order to reach higher S/N ratios.[17] In fact, it is known that both biological and non-biological noises can negatively affect the recording of neural signals.[17c] Thus, in general, the reduction of the impedance of the microelectrode by electrodepositing PEDOT based conductive films will produce a significant reduction of the thermal noise, resulting in an improved neural recording sensitivity. From the time integral of the cathodic current by CV analysis (typical trace reported in Figure S4) the CSC of 3.2 ± 0.2 mC cm^{-2} and 2.6 ± 0.2 mC cm^{-2} (n = 3) were calculated for PEDOT-TUDCA and PEDOT-DEX, respectively (see experimental section for details).[17a] These values are in accordance with CSC data recently reported by C. Boehler *et al*. for neural implants coated with PEDOT-DEX for a chronic in vivo neural recording study.[4a]

Equivalent Circuit Modelling

To gain insights on the charge transport dynamics within both PEDOT-TUDCA and PEDOT-DEX films, circuit modelling was used to fit experimental EIS data in the frequency interval of 10^5-0.05 Hz. The model proposed by Danielson *et al*. provided the best fit to experimental data ($\chi^2 \sim 10^{-4}$). This model is represented by a solution resistance (R_s) in series with a charge transfer element (a charge transfer resistance R_{CT} in parallel with a capacitor C), the double layer capacitance represented by a constant phase element (CPE) and a finite-length Warburg impedance (T) that describes processes dominated by ion diffusion (Figure 4a).[4b,18]

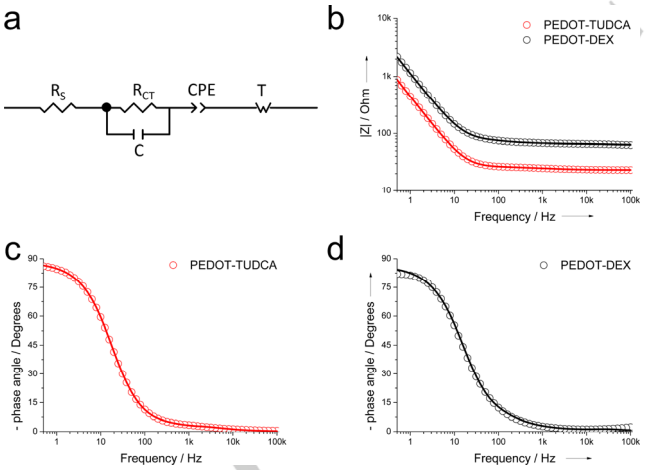

Figure 4. Representative EIS circuit model for PEDOT-TUDCA and PEDOT-DEX (experimental data as circles, theoretical data as lines): a) circuit model, b) Bode module, c) and b) Bode phase plots.

In Figure 4, experimental and theoretical Bode module (4b) and Bode phase (4c,d) plots are reported, respectively. It can be observed the typical *near Ohmic* behaviour of PEDOT coatings that extends the interval of frequency independent impedance from 10^5 to 10^2 Hz, for both PEDOT-TUDCA and PEDOT-DEX. It has been reported that improved charge transport dynamics along the conductive film leads to a wider range of frequency independent impedance.[19] From this perspective, both PEDOT-TUDCA and PEDOT-DEX exhibit similar behaviour. The relevant parameters obtained from EIS fitting are reported in Table 1 (a more detailed Table S1 is reported in the supporting information)

Table 1. Relevant parameters obtained from EIS circuit model (from a set of 3 different PEDOT-TUDCA and PEDOT-DEX electrodes, respectively) .

Sample	R_S Ω	τ µs	Q_0 10^{-5} Ss^n	n	R_D[a] (Ω)	C_{LF}[b] 10^{-5} F
PEDOT-TUDCA	21 ± 2	32 ± 13	55 ± 4	0.97	6 ± 2	45 ± 2
PEDOT-DEX	40 ± 1	4.5 ± 0.9	24 ± 2	0.93	21 ± 8	22 ± 2

[a] see ref. 22 [b] see ref. 20.

Solution resistance is defined as $R_s = \rho(l/A)$, where *l* is the length, *A* is the area of the electrode and ρ the solution resistivity. A contribution from the Ohmic resistance of PEDOT films to R_s cannot be excluded a priori, although R_s is dominated by the resistance of the electrolyte solution.[20] Therefore, affording that both *l* and the ionic concentration of the electrolyte are constant during EIS experiments, the higher R_s of PEDOT-DEX (~ 40 Ω), can be explained in terms of a reduced electroactive surface area and/or a lower electronic conductivity of PEDOT-DEX, with respect to PEDOT-TUDCA (R_s ~ 20 Ω). As far as the charge transfer process is concerned (see Figure 4a), the fitting provided two different time constant ($\tau = R_{CT}C$) in the order of 4.5 µs and 32 µs for PEDOT-DEX and PEDOT-TUDCA, respectively. The nature of this process has been ascribed mainly to the charge transfer at the interface PEDOT||electrode, electrolyte||PEDOT as well as to charge transport along the conductive film.[21] The constant phase element CPE reflects the behaviour of a non-ideal capacitor, which is mainly due to the roughness of the electrode material, including PEDOT coatings.[22] Its impedance is defined as $1/Z_{CPE} = Q_0(j\omega)^n$, where the physical meaning of the term Q_0 can be ascribed to the electrode capacitance, whereas the exponent n relates to the roughness of the electrode. The higher CSC obtained for PEDOT-TUDCA from CV characterization is in accordance with the higher Q_0 and experimental low frequency capacitance C_{LF} ($-Z_j = 1/\omega C_{LF}$, $f \rightarrow 0.1$ Hz) reported in Table 1. Therefore, the improved higher capacitance of PEDOT-TUDCA, is detrimental in lowering its total impedance if compared to PEDOT-DEX coatings. Moreover, the reduced diffusional resistance R_D of the Warburg impedance ($Z_D = R_D\coth(j\omega\tau)^{1/2})/(j\omega\tau)^{1/2}$) is consistent with a less restricted ion transport in the PEDOT-TUDCA film (see Table 1).[22] To sum up, equivalent circuit analysis is consistent with an increased film thickness that leads to higher

capacitance of PEDOT-TUDCA, as well as to a different surface morphology between PEDOT-TUDCA and PEDOT-DEX.

Optical and Surface Characterization

The surface morphology of PEDOT-TUDCA and PEDOT-DEX films was characterized by means of scanning electron microscopy (SEM) and atomic force microscopy (AFM). As visible in the SEM images of Figure 5a and 5b both coatings exhibit a granular-like morphology, which is typically observed for electropolymerized PEDOT in aqueous/surfactant electrolytes.[4b,13,21,23]

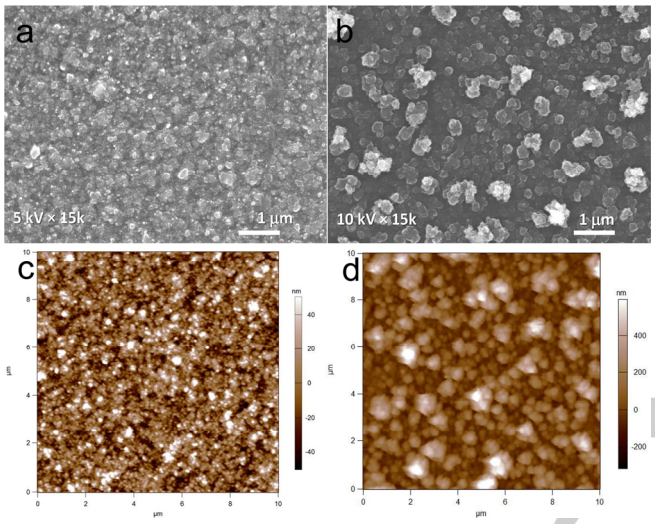

Figure 5. SEM and AFM surface morphology analysis for PEDOT-TUDCA (a,c) and PEDOT-DEX (b,d).

It is noteworthy that a transition from globular to rod-like and fibrous morphology was reported for PEDOT overoxidation.[24] However, PEDOT-TUDCA exhibits a more compact surface with smaller average grain size of ~100 nm, whereas that of PEDOT-DEX is ~300 nm. These numbers are confirmed by AFM measurements (Figure 5c and 5d), which also provides the height of the grains. This is likely due to a higher tendency of PEDOT-TUDCA oligomers to precipitate on the electrode surface leading to grains of smaller size, when compared to PEDOT-DEX coating, in accordance with the mechanism proposed for the polymer growth.[16]

Table 2. Relevant parameters obtained from AFM analysis.

Sample	Film thickness t (nm)	Top roughness S_q (nm) [a]	Grain size d (nm) [b]
PEDOT-TUDCA	930 ± 50	23 ± 5	100 ± 50
PEDOT-DEX	520 ± 50	140 ± 30	300 ± 60

[a]50 µm scan size; [b] 10 µm scan size.

AFM analysis carried out across scratches hand-made with sharp tweezers also allowed to confirm an increased thickness of up to 930 nm for PEDOT-TUDCA films, with respect to the value of 520 nm for PEDOT-DEX, as suggested by electrochemical characterization.

Moreover, higher roughness S_q was observed for PEDOT-DEX films, in accordance with the results obtained from the EIS circuit model. In particular, the CPE exponent n was calculated for PEDOT-DEX in the order of 0.93 reflecting a less ideal surface, whereas for PEDOT-TUDCA a value of 0.97 was obtained, closer to the ideal value of n = 1 for a pure capacitor.[22]

Adhesion tests were performed in order to assess whether the increased thickness of PEDOT-TUDCA may facilitate film delamination, with respect to the thinner PEDOT-DEX films. For this purpose, we employed a modified American Society for Testing and Materials standard test method for measuring adhesion by test tape, that was reported in literature as an effective tool to evaluate the delamination due to mechanical stress of conductive polymer films.[4b,25] EIS was collected before and after the adhesion test in order to quantify any possible increased resistivity due to the film delamination. Optical images confirmed the stability of PEDOT-TUDCA whereas PEDOT-DEX showed randomly distributed patches which are consistent with partial coating degradation (see Figure 6).

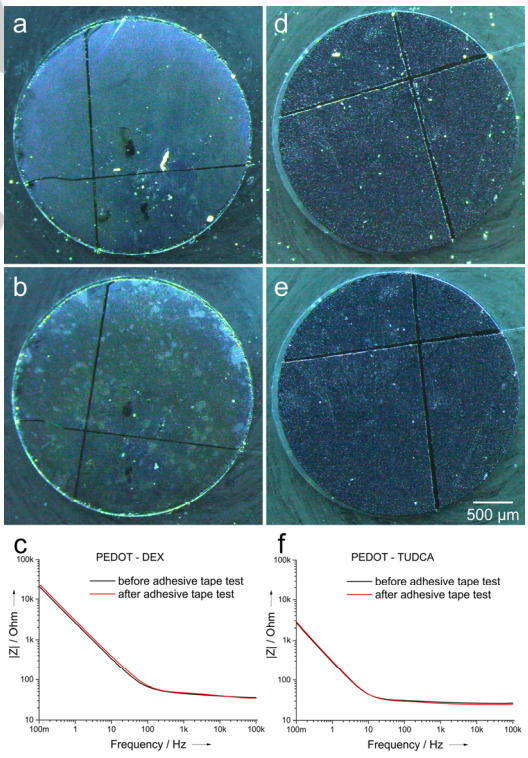

Figure 6. optical images of PEDOT-DEX and PEDOT-TUDCA before (a and d, respectively) and after (b and e, respectively) the adhesive tape test. Impedance spectra of (c) PEDOT-DEX and (f) PEDOT-TUDCA, before and after adhesive tape test.

EIS was performed before and after the test in order to quantify the extent of delamination. Both coatings preserved similar

resistive behaviour in the frequency range of 10^5-100 Hz, but an increase of diffusional capacitance C_{LF} for PEDOT-TUDCA was estimated in the order of 5% whereas for PEDOT-DEX a value of 13% was obtained. This is consistent with partial thinning related to the loss of material from the outermost surface rather than delaminating from the substrate, and this phenomenon is more pronounced for PEDOT-DEX. Therefore, adhesion test suggests that the higher thickness does not impair the mechanical adhesion of PEDOT-TUDCA with the underlying substrate, with respect to PEDOT-DEX.

X-ray photoelectron spectroscopy (XPS) was adopted to confirm the presence of the dopant TUDCA within the PEDOT backbone. The S(2p) core-level spectra from films of PEDOT-TUDCA (Figure 7) is dominated by two distinct doublets at the binding energy of 163.8 ± 0.2 eV and 167.6 ± 0.2 eV which can be ascribed to the sulfur atoms of PEDOT and the SO_3^- groups of TUDCA, respectively.[17b,26] The supplementary doublet at higher binding energy (~169 eV) has been ascribed to protonated sulfonate groups SO_3H due to the release of protons during EDOT polymerization.[16,26a] The *doping-ratio*, a parameter that defines the degree of dopant incorporation, can be estimated by the ratio between the SO_3^- groups of TUDCA and the EDOT sulfur atoms, as obtained by quantitative XPS analysis. In particular, the relative amounts (% molar) of the two S species were calculated in the order of 79.7 (PEDOT) and 18.6 (TUDCA-SO_3^-) leading to a doping ratio of 0.23, which falls within the typical range of 0.2-0.4 for electrochemically prepared PEDOT composite films.[27] This is consistent with one TUDCA-SO_3^- dopant for four-five EDOT units.

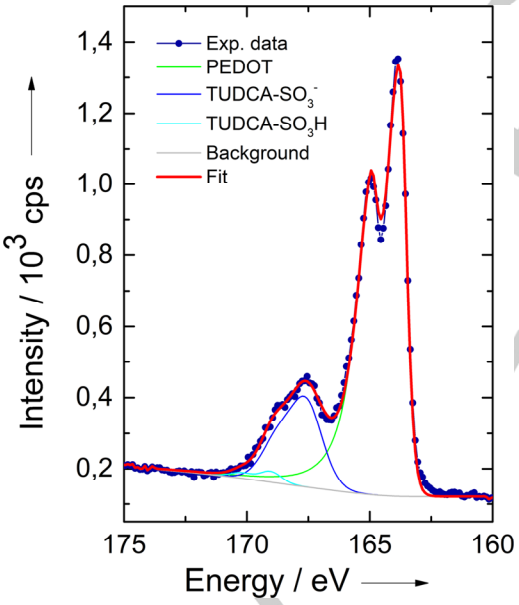

Figure 7. Typical XPS results collected on PEDOT-TUDCA films over the S 2p binding energy range.

In Vitro Release Study

Cyclic voltammetry (CV) was used to promote an electrochemically controlled delivery of TUDCA. The cathodic potential of -1V (Vs Ag/Ag^+) was chosen in order to assess a complete reduction of the conductive film, in accord with the CV analysis of PEDOT-TUDCA that shows a pronounced reduction peak at -0.65V (see Figure S6). In Figure 8 we outlined the comparison between the release observed for electrodes subjected to a progressive number of CV cycles (active release) and electrodes immersed in the electrolyte during the same time-windows (see details in the experimental section). Both active and passive releases exhibited an initial burst phase, but it is evident (Figure 8a) that there is a significant electrochemical contribution to the rate of release, as well as to the total mass delivered by the active mode. In particular, during 360 minutes (500 CV cycles) the electrodes subjected to active release provided a total amount in the order of 305 ± 6 nmol cm^{-2} that exceeded the cumulative mass spontaneously released (109 ± 29 nmol cm^{-2}). After removing the electrochemical stimulation, the passive release of TUDCA was monitored from all electrodes over a period of 7 days (even if in some cases the release extended up to 9-10 days). During this time window the total amount of released TUDCA increased progressively from 318 nmol cm^{-2} to 340 nmol cm^{-2} for the electrodes that were previously subjected to the electrochemical activation, and from 125 nmol cm^{-2} to 152 nmol cm^{-2} for the untreated ones (Figure 8b). This result further corroborates the electrochemical contribution to the active release. It is important to note that the electrochemical triggers not only promote a faster release during the analysed 500 CV scans but also influence the total drug mass delivered. In fact, the total release provided by active control was quantified in the order of 340 ± 44 nmol cm^{-2} whereas a lower value of 152 ± 45 nmol cm^{-2} was observed for the passive release. It is known that conductive polymers act as electrochemical actuators when subjected to potential sweeping, thereby producing a change in their volume.[28] Therefore, the improved mass delivery obtained with the active control is consistent with an increased accessible area of PEDOT-TUDCA by the electrolyte, due to the expansion and contraction (actuation) of the polymeric film. It is noteworthy that uncontrollable spontaneous release is typically observed for ionically incorporated drugs within PEDOT or conductive polymer based coatings.[29] Several approaches may be adopted to slow down the rate of the TUDCA release. For example, Boehler et al. reported that the rate of DEX release was significantly reduced when a second layer of PEDOT-PSS was electrodeposited on the top of the PEDOT-DEX substrate, thereby forcing the drug to diffuse through the stacked layer before it reaches the bulk electrolyte.[29a] Alternatively, the covalent approach that we reported recently may be suitable for this purpose as well.[6] Despite TUDCA was reported to exert anti-inflammatory effect in microglia, the biologically active concentration of this drug that should be released from a localized drug delivery system was not evaluated so far.[8] For example, a local release of DEX in the order of 0.5 μg cm^{-2} was established to provide a therapeutic effect toward acute neural inflammation reduction.[30]

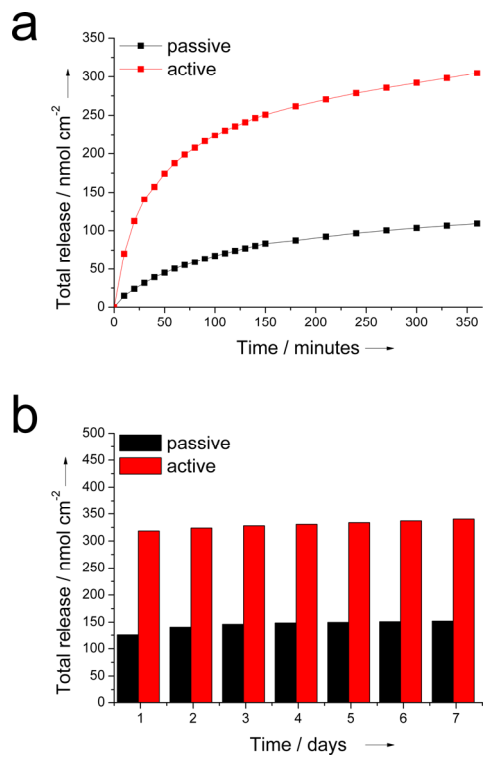

Figure 8. Cumulative mass of TUDCA released from glassy carbon electrodes (area 0.07 cm^2) coated with PEDOT-TUDCA: a) active Vs passive and b) spontaneous after removal of electrochemical triggers. The results represent the mean from two different experiments.

Assuming that the total amount of incorporated TUDCA is in the order of 340 nmol cm^{-2}, as obtained from active control, the kinetic and mechanism of release can be evaluated by modelling experimental data with the Avrami's equation $X = 1 - \exp(-kt^n)$: where X is the molar fraction of released drug, *K* and n express the magnitude of release and are empirically determined. [31] In particular, it has been reported that Avrami's equation fits well diffusion-controlled and potential-assisted drug-release data, particularly for ion exchange release as well as conductive polymers. [31a] Thus, we have used this model to fit experimental data obtained from active release (MATLAB software, MathWorks R18b). We found that this equation give a good fit for the first 70% of release, providing R^2 values of 0.998 and 0.999 for active and passive release, respectively. In Figure 9 we report experimental and theoretical release profiles, as derived by Avrami's equation. The Avrami's parameter n is related to the release mechanism and, in particular, n = 1 is ascribed to first-order kinetics whereas n = 0.54 corresponds to diffusive release.[31] The values of n = 0.61 and 0.64 were obtained for experimental data acquired in active and passive mode, respectively, suggesting that the release of TUDCA is dominated by a diffusion kinetic in both cases. As expected, the higher rate release constant k of 0.065 min^{-1} obtained for the active mode, corroborates the implication of the electrochemically promoted delivery over the passive release (k = 0.011 min^{-1}).

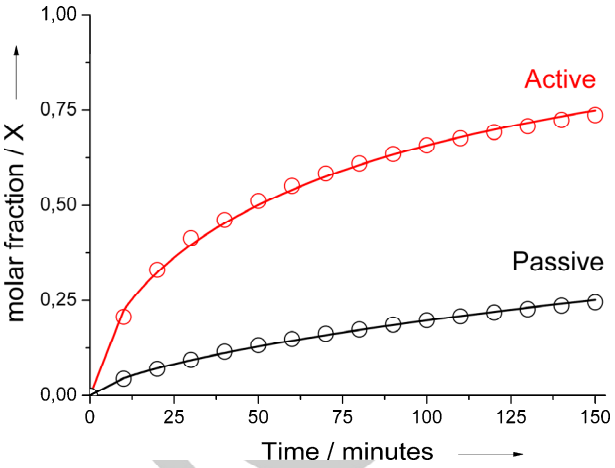

Figure 9. Release mechanism analysis: experimental and fitted by Avrami's model.

Cell Viability

Finally, cell viability assay was performed at different time point (1, 3, and 7 days) on PEDOT-TUDCA, PEDOT-DEX substrates to evaluate the cell survival as well as the cytocompatibility of the coatings. In agreement with the international standard ISO10993 and with what is widely reported in literature, we used fibroblast cells to provide the cytotoxicity evaluation of the new material.[32] This analysis represents the first important step that can be performed to gain insights on the biocompatibility of a new material.[33] PEDOT-PSS was also included due to its well-known biocompatibility.[34] After one day of culture, in all cases the cells were able to adhere to the substrate, although a slightly increased cell adhesion was observed for PEDOT-DEX substrate, consistent with its higher roughness and/or grain size.[35] In fact, according to AFM characterization the roughness of PEDOT-DEX was estimated in the order of 140 nm, whereas for PEDOT-TUDCA a value of 23 nm was observed (see Table 2). Nevertheless, all substrates were able to grow up and proliferate progressively from the third to the seventh day of culture, forming a thick layer of living cells (Figure S7). PEDOT-TUDCA appears to be the best long-term growth substrate, whereas in contact with PEDOT-PSS, cell viability appears to be lower for the entire duration of the experiment, as outlined in Figure 10. This result makes PEDOT-TUDCA a new promising material also in terms of biocompatibility.

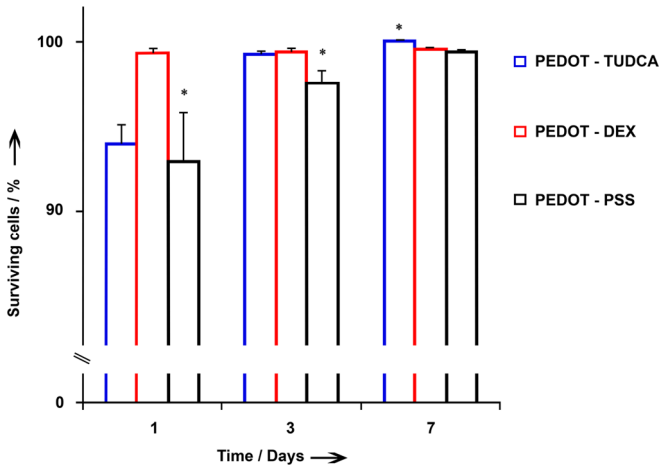

Figure 10. Quantitative analysis of the viability of fibroblasts cells cultured on PEDOT-TUDCA (blue bars), PEDOT-DEX (red bars), PEDOT-PSS (gray bars) substrate at 1, 3, and 7 days in vitro. The percentages of surviving cells (means ± ER) were calculated based on the ratio of total (Hoechst-positive) nuclei minus PI-positive nuclei divided by the total nuclei. *: p-value < 0.05 (statistical significance applies at each 1,3 and 7 days/group, independently).

Conclusions

In summary, the bile acid TUDCA has been successfully incorporated within PEDOT coatings and a substantial electrochemically controlled release was obtained. The new PEDOT-TUDCA exhibited promising electrochemical as well as biocompatibility properties even when compared to classic PEDOT-DEX coatings with ionically incorporated drug. These new findings, together with recent literature reporting possible therapeutic implications for inflammatory CNS diseases, provide helpful tools for the rational design of advanced localized drug delivery systems using the natural bile acid TUDCA. Neuroscience is among those application that may benefit from this new PEDOT-TUDCA composite material. In fact, neural probes coated with PEDOT-TUDCA could offer a new possibility of modulating the brain tissue inflammation while preserving recording/stimulating capability. Nevertheless, further *in-vivo* experiments should be performed to establish and optimize the amount of bioactive drug locally delivered by PEDOT-TUDCA coatings in order to guarantee neuroprotective properties.

Experimental Section

Materials

All chemicals including 2,3-Dihydrothieno[3,4-b]-1,4-dioxin (EDOT) and Dexamethasone phosphate (Dex-P) were from Sigma Aldrich (Italy), except otherwise specified. Commercially available glassy carbon (GC) electrodes (diam. 3 mm) were provided by IJ Cambria Scientific Ltd. Ultrapure water (Milli-Q, Millipore, USA) was used for this study. Tauroursodeoxycholic acid was kindly supplied from ICE SpA. Italy. Tauroursodeoxycholic acid, sodium salt was purchased from Glentham Life Sciences Ltd, United Kingdom. All experimental data were elaborated using the software OriginPro v8.

Electrodepositions and Electrochemical Characterization

Cyclic voltammetry (CV), electrochemical impedance spectroscopy (EIS) and coating electrodepositions were carried out using a Reference 600 potentiostat (Gamry Instruments, USA) connected to a three-electrode electrochemical cell with a commercial glassy carbon (3 mm diam.) set as the working electrode, a Pt wire as a counter electrode and a Ag/AgCl reference electrode (+0.197 V vs NHE). EIS were performed by superimposing a voltage sine wave modulation (10 mV RMS amplitude, 0 V potential applied) within the frequency interval of 10^5 - 0.1 Hz. CSCc were calculated from the time integral of the cathodic current of cyclic voltammogram over the potential range of -0.6V-0.8V, which is within the water electrolysis window.[17a] The electrochemical characterizations were collected in 1M PBS aqueous solution. The software ZSimpWin V 3.2 (EChem Software) was used for equivalent circuit modeling of EIS data and χ^2 values in the range of 10^{-4}–10^{-5} were used to estimate the goodness of the fit. The electrochemical deposition was carried out in potentiodynamic mode, with a scan rate of 100 mV s^{-1}, for a total of 20 cycles. The potential range of 0 V-1.2 V was used for preparation of PEDOT-TUDCA and PEDOT-DEX. A solution of EDOT (0.01N) and the commercially available sodium salt of TUDCA (0.02N) was used for the deposition of PEDOT-TUDCA. Similarly, the preparation of PEDOT-DEX was achieved by using the dopant DEX-P (0.02N) dissolved in water.

In Vitro TUDCA release

The release of TUDCA from GC coated with PEDOT-TUDCA was conducted in saline solution at 25°C. The experiments were performed in duplicated and the data are presented as the average of all the samples analyzed. Active release from was monitored by subjecting the immersed electrodes to a well-defined number of voltammetric cycles in the potential range of +0.5/-1V at the scan rate of 100 mV s^{-1}. Initially, the number of cycles was set at 10. After removing the electrochemical stimulation, the electrodes were kept immersed in the solution for a total time of ten minutes (taking into account that the voltage excursion is equal to 3V, a total time of 5 minutes is needed to complete a full 10 cycles trigger). Passive release was obtained by immersing the PEDOT-TUDCA electrodes during the same time window without applying any external electrochemical trigger. For each reading, the release solution was removed and stored at -20°C and the electrode was immersed in a fresh saline solution. After 150 cycles, corresponding to the total time of 150 minutes, the electrodes were subjected to further five set of 50 cycles, and the release solution was refreshed after a total time of 30 minutes/step. Subsequently, all the electrodes were subjected to passive release for a total time of 10 days: in this case the release solution was renewed every 24 hours. Evaluation of the release amount of TUDCA was performed by HPLC analysis (see supporting information for details).

Keywords: Electrochemistry • Drug delivery • Conductive polymers • Electrodeposition • Neural recording

[1] a) K. J. Ressler, H. S. Mayberg, *Nat. Neurosci.* **2007**, *10*, 1116-1124; b) A. M. Owen, *Neuroscientist* **2004**, *10*, 525-537; c) M. A. Nicolelis, *Nat. Rev. Neurosci*. **2003**, *4*, 417-422.

[2] a) R. J. Vetter, J. C. Williams, J. F. Hetke, E.A. Nunamaker, D. R. Kipke, *Biomed. Eng. IEEE Trans.* **2004**, *51*, 896–904; b) J. C. Williams, J. A. Hippensteel, J. Dilgen, W. Shain, D.R. Kipke, *J. Neural. Eng.* **2007**, *4*, 410-423; c) T. Saxena, L. Karumbaiah, E. A. Gaupp, R. Patkar, K. Patil, M. Betancur, G. B. Stanley, R. V. Bellamkonda, *Biomaterials* **2013**. 34, 4703-4713; d) R. Biran, D.C. Martin, P. A. Tresco, *Exp. Neurol.* **2005**, *195*, 115-26.

[3] a) Z. Aqrawe, J. Montgomery, J. Travas-Sejdicc, D. Svirskis, Sens. Actuators B **2018**, *257*, 753–765; b) R. Green, M. R. Abidian, *Adv. Mater.* **2015**, *27*, 7620–7637.

[4] a) C. Boehler, C. Kleber, N. Martini, Y. Xie, I. Dryg, T. Stieglitz, U. G. Hofmann, M. Asplund, *Biomaterials* **2017**, *129*, 176–187; b) E. Castagnola, S. Carli, M. Vomero, A. Scarpellini, M. Prato, N. Goshi, L. Fadiga, S. Kassegne, D. Ricci, *Biointerphases* **2017**, *12*, 031002; c) N. A. Alba, Z. J. Du, K. A. Catt, T. D. Y. Kozai, X. T. Cui, *Biosensors* **2015**, *5*, 618–646.

[5] a) D. Svirskis, J. Travas-Sejdic, A. Rodgers, S. Garg, *J. Controlled Release* **2010**, *146*, 6–15; b) D. Uppalapati, B. J. Boyd, S. Garg, J. Travas-Sejdic, D. Svirskis, *Biomaterials* **2016**, *111*, 149–162; c) B. Massoumi, A. Entezami, J. Bioact. Compat. Polym. **2002**, *17*, 51–62.

[6] S. Carli, C. Trapella, A. Armirotti, A. Fantinati, G. Ottonello, A. Scarpellini, M. Prato, L. Fadiga, D. Ricci *Chem. Eur. J.* **2018**, *24*, 10300-10305.

[7] a) N. Yanguas-Casás, M. A. Barreda-Manso, S. Pérez-Rial, M. Nieto–Sampedro, L. Romero-Ramírez, *Mol Neurobiol* **2017**, *54*, 6737–6749; b) N. Yanguas-Casás, M. A. Barreda-Manso, S. Pérez-Rial, M. Nieto–Sampedro, L. Romero-Ramírez, *J. Neuroinflamm*. **2014**, *11*: 50; c) K. R. Gronbeck, C. M. P. Rodrigues, J. Mahmoudi, E. M. Bershad, G. Ling, S. P. Bachour, A. A. Divani, *Neurocrit. Care* **2016**, *25*, 153–166; d) S. Vang, K. Longley, C. J. Steer, W. C. Low, *Global Adv Health Med.* **2014**, *3*, 58-69; e) J. D. Amaral, R. J. S. Viana, R. M. Ramalho, C. J. Steer, C. M. P. Rodrigues, *J. Lipid Res.* **2009**, 50, 1721-1734.

[8] a) A. Noailles, L. F. Sánchez, P. Lax, N. Cuenca, *J. Neuroinflamm*. **2014**, *11*, 1-22 (article 186); b) S.S. Joo, T.J. Won, D.I. Lee, Arch. Pharm. Res. **2004**, *27*, 954–960

[9] J. J. G Marin, *World J Gastroenterol* **2009**, *15*, 804-816.

[10] S. Baek, R. A. Green, L. A. Poole-Warren, *J. Biomed. Mater. Res. Part A* **2014**, *102A*, 2743-2754.

[11] V. Castagnola, C. Bayon, E. Descamps, C. Bergaud, Synth. Met. 2014, 189, 7 ‑16.

[12] F. G. Bordwell, *Acc. Chem. Res.* **1988**, *21*, 456-463.

[13] N. Sakmeche, S. Aeiyach, J. A. Jaques, M. Jouini, J. C. Lacroix, P. C. Lacaze, *Langmuir* **1999**, *15*, 2566−2574.

[14] J. M. Valderrama, P. Wilde, A. Macierzanka, A. Mackie, *Adv Colloid Interface Sci* **2011**,*165*, 36-46.

[15] a) S. Carli, L. Casarin, G. Bergamini, S. Caramori, C. A. Bignozzi, *J. Phys. Chem. C* **2014**, *118*, 16782 ‑16790; b) H. Randriamahazaka, V. Noël, C. Chevrot, *J. Electroanal. Chem.* **1999**, *472*, 103‑ 111; c) J. Heinze, A. Rasche, M. Pagels, B. Geschke, *J. Phys. Chem. B* **2007**, *111*, 989-997.

[16] J. Roncali, *Chem. Rev.* **1992**, *92*, 711-738.

[17] a) S. F. Cogan, *Annu. Rev. Biomed. Eng.* **2008**, *10*, 275–309; b) S. Carli, L. Lambertini, E. Zucchini, F. Ciarpella, A. Scarpellini, M. Prato, E. Castagnola, L. Fadiga, D. Ricci, *Sens. Actuator B-Chem*. **2018**, *271*, 280-288; c) M. E. J. Obien, K. Deligkaris, T. Bullmann, D. J. Bakkum, U. Frey, *Front. Neurosci.* **2015**, *8*, 1-30 (article 423); d) J. E. Ferguson, C. Boldt, A. D. Redish, *Sens. Actuator A: Phys.* **2009**, *156*, 388–393.

[18] P. Danielsson, J. Bobacka, A. Ivaska, *J. Solid State Electrochem*. **2004**, *8*, 809-817.

[19] M. Ovadia, D. H. Zavitz, J. F. Rubinson, D. Park, H. A. Chou, *Chem. Phys. Lett*. **2006**, *419*, 277–287.

[20] J. Bobacka, A. Lewenstam, A. Ivaska, *J. Electroanal. Chem.* **2000**, *489*, 17–27.

[21] S. Carli, E. Busatto, S. Caramori, R. Boaretto, R. Argazzi, C. J. Timpson, C. A. Bignozzi, *J. Phys. Chem. C* **2013**, *117*, 5142 ‑5153;

[22] I. Barsoukov, J.R. Macdonald in *Impedance Spectroscopy: Theory Experiment and Applications*, 2nd ed., John Wiley & Sons Inc., Hoboken, NJ, 2005.

[23] J. Xia, N. Masaki, K. Jiang, S. Yanagida, *J. Mater. Chem.* **2007**, *17*, 2845‑2850

[24] a) S. Patra, K. Barai, N. Munichandraiah, *Synth. Met.* **2008**, *158*, 430-435; b) X. Du, Z. Wang, *Electrochim. Acta* **2003**, *48*, 1713-1717.

[25] J. A. Goding, A. D. Gilmour, J. P. Martens, L. A. Poole-Warren, R. A. Green, *J. Mater. Chem. B* **2015**, *3*, 5058-5069.

[26] a) G. Zotti, S. Zecchin, G. Schiavon, F. Louwet, L. Groenendaal, X. Crispin, W. Osikowicz, W. Salaneck, M. Fahlman, *Macromolecules,* **2003**, *36,* 3337-3344; b) G. Greczynskia, Th. Kuglerb, M. Keila, W. Osikowicza, M. Fahlmanc, W. R. Salaneck, *J. Electron Spectrosc. Relat. Phenom.* **2001**, *121*, 1 –17; c) K.Z. Xing, M. Fahlman, X. W. Chen, O. Inganäs, W. R. Salaneck, *Synth. Met.* **1997**, *89*, 161-165.

[27] a) R. A. Green, N. H. Lovell, L. A. Poole-Warren, *Biomaterials* **2009**, *30*, 3637–3644; b) J. M. Fonner, L. Forciniti, H. Nguyen, J. D. Byrne, Y.-F. Kou, J. Syeda-Nawaz and C. E. Schmidt, *Biomed. Mater.* **2008**, *3*, 034124.

[28] a) Q. B. Pei, O. Inganas, *Adv. Mater.* **1992**, *4*, 277-278; b) T. F. Otero, M. T. Cortes, *Adv. Mater*. **2003**, *15*, 279-282; c) E. Smela, O. Inganas, I. Lundstrom, *Science* **1995**, *268*, 1735-1738.

[29] a) C. Boehler, M. Asplund, *J. Biomed. Mater. Res. Part A* **2015**, *103*, 1200 – 1207; b) C. L. Kolarcik, K. Catt, E. Rost, I. N. Albrecht, D. Bourbeau, Z. Du, T. D. Y. Kozai, X. Luo, D. J. Weber, X. T. Cui, *J. Neural Eng.* **2015**, *12*, 016008; c) K. Krukiewicz, P. Zawisza, A. P. Herman, R. Turczyn, S. Boncel, J. K. Zak, *Bioelectrochemistry* **2016**, *108*, 13-20.

[30] Y. Zhong, R. V. Bellamkonda, *Brain Res*. **2007**, *1148*, 15‑ 27.

[31] a) E. Shamaeli, N. Alizadeh, *Int. J. Pharm.* **2014**, *472*, 327–338; b) A. T. Lorenzo, M. L. Arnal, J. Albuerne, A. J. Müller, *Polym. Test.* **2007**, *26*, 222–231.

[32] a) T. Geninatti, G. Bruno, B. Barile, R. L. Hood, M. Farina, J. Schmulen, G. Canavese, A. Grattoni, *Biomed Microdevices*. **2015**, *17*, 24; b) A. Gupta, P. Majumdar, J. Amit, A. Rajesh, S. B. Singh, M. Chakraborty, *Trends Biomater. Artif. Organs* **2006**, *20*, 84-89; c) J. Chłopek, B. Czajkowsk, B. Szaraniec, E. Frackowiak, K. Szostak, F. Béguin, *Carbon* **2006**, *44*, 1106-1111; d) International Standard **ISO 10993-5:2009** *Biological evaluation of medical devices-Part 5: Tests for in vitro* cytotoxicity.

[33] W. Li, J. Zhou, Y. Xu, *Biomed. Rep.* **2015**, *3*, 617–620.

[34] M. Yazdimamaghani, M. Razavi, M. Mozafari, D. Vashaee, H. Kotturi, L. Tayebi, *J. Mater. Sci.- Mater.Med*. **2015**, *26*,1-11(article 274).

[35] M. Lampin, R. Warocquier-Clerout, C. Legris, M. Degrange, M. F. Sigot-Luizard, J. *Biomed. Mater. Res.*, **1997**, *36*, 99-108.

10.1002/chem.201805285

WILEY-VCH

Layout 2:

FULL PAPER

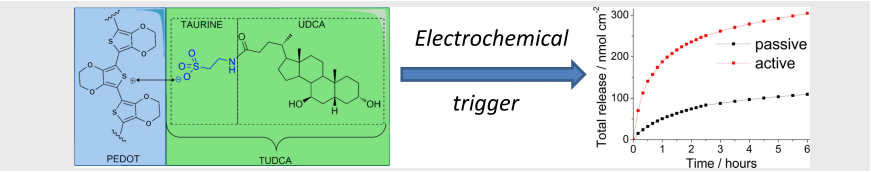

From bears to brain. The Food and Drug administration-approved hydrophilic bile acid Tauroursodeoxycholic acid (TUDCA) was successfully incorporated in electrodeposited PEDOT films. This study was aimed to the realization of a new PEDOT-TUDCA composite material that may result as a potential substitute of the synthetic glucocorticoids for localized drug delivery system in neuroscience applications.

Stefano Carli, Giulia Fioravanti, Andrea Armirotti, Giuliana Ottonello, Mirko Prato, Marco Salerno, Francesca Ciarpella, Alice Scarpellini, Daniela Perrone, Elena Marchesi, Davide Ricci, Luciano Fadiga.*

*Author(s), Corresponding Author(s)**

Page No. 1– Page No.8

A New Drug Delivery System based on Tauroursodeoxycholic Acid and PEDOT